Temporal variation of ^{129}I and ^{127}I in aerosols from Xi'an, China: influence of East Asian monsoon and heavy haze events

Luyuan Zhang [1,2*], Xiaolin Hou [1,2,3], Sheng Xu [4], Tian Feng [1], Peng Cheng [1], Yunchong Fu [1], Ning Chen [1]

[1]State Key Laboratory of Loess and Quaternary Geology, Shaanxi Key Laboratory of Accelerator Mass Spectrometry Technology and Application, Xi'an AMS Center, Institute of Earth Environment CAS, Xi'an 710061, China

[2]Center for Excellence in Quaternary Science and Global Change, Chinese Academy of Sciences, Xian 710061, China

[3]Center for Nuclear Technologies, Technical University of Denmark, Risø Campus, Roskilde 4000, Denmark

[4]Institute of Surface-Earth System Science, Tianjin University, Tianjin 300072, China

Correspondence to: Luyuan Zhang (zhangluyuan.118@163.com)

The supplementary information includes seven figures and two tables.

SI-1 Determination of ^{129}I and ^{127}I in aerosol samples

S1.1 Aerosol sampling

The aerosol samples were collected by a high-volume sampler onto glass fibre filters (200 mm×250 mm, Tianhong Instrument Ltd., Wuhan, China). The flow rate is 1.5 m^3 min^{-1} and the sample duration was 24 h for each filter with air flux of 2100 m^3. The sampler is installed on the roof of the Xi'an AMS Centre in Xi'an, China (34°13'25"N, 109°0'0"E) with an elevation of 440 m above mean sea level (Fig.1). Xi'an, located in the Guanzhong basin, is the largest city in northwest China with a population of 9.9 million. The basin is nestled between the Qin Ling in the south and the Loess Plateau in the north, and is warm temperate zone with semihumid continental monsoon climate (Fig.1b).

S1.2. Iodine isotopies analysis

68 aerosol filters, about four filter samples in each month, were selected for measurement of iodine isotopes. Each filter represents one day information. Half of one filter with air flux of about 1000 m^3 was analysed for ^{129}I, and the other half was reserved for other use. Iodine was separated from the aerosol filter using pyrolysis and AgI-AgCl coprecipitation in combination with accelerator mass spectrometry (AMS) for measurement, as described elsewhere (Zhang et al., 2018b). In brief, the aerosol samples were placed into a corundum boat. ^{125}I in the form of iodide was added for calculation of chemical yield. Iodine in the samples was released as gaseous form at high temperature in the atmosphere of nitrogen and oxygen gases in a tube furnace (Hou et al., 2010). The released iodine was trapped into a solution containing 0.5 mol L^{-1} NaOH and 0.02 mol L^{-1} $NaHSO_3$. An aliquot of solution (1.0 mL) was taken for determination of ^{127}I using ICP-MS (Agilent 8800, USA). Another 1.0 mL solution was taken to a tube and counted for ^{125}I using a NaI gamma counter (Model FJ2021, Xi'an Nuclear Instrument Factory, China) to calculate the chemical yield of iodine during combustion. After gamma measurement, 0.2 mg ^{127}I carrier was added to the trap solution. For procedure blank samples, 0.5 mg chloride (as NaCl) was added. 1 mL of 0.5 M $NaHSO_3$ was used to reduce iodate to iodide. The solution was adjusted to pH < 2 by 3 M HNO_3. 1 mL 0.5 M $AgNO_3$ solution was directly added to the solution to precipitate iodine as AgI-AgCl coprecipitation. The formed AgI-AgCl precipitate was washed once with 3 M HNO_3 to remove Ag_2SO_3 and Ag_2SO_4, then washed with deionized water once and 5-20% ammonium hydroxide once to remove excessive AgCl, and finally rinsed twice with deionized water. After centrifugation, the AgI-AgCl

coprecipitate was ready for AMS measurement. The procedural blank was prepared using a blank glass fibre filter with the same procedure as that for samples.

S1.3 AMS and ICP-MS determination of ^{129}I and ^{127}I

The sample AgI-AgCl coprecipitate were completely dried at 70°C, then mixed with Nb metal powder (99.9%, 325 mesh, Alfa Aesar, USA) in a mass ratio of 1:5 and pressed into bronze target holders. ^{129}I in the target was measured using a 3MV AMS in the Xi'an AMS Centre (Hou et al., 2010). A voltage of 2.5 MV is applied for measurement of $^{129}I/^{127}I$ ratio. The +5 charge state of iodine ion is selected and extracted from the accelerator by a magnetic analyser. $^{129}I/^{127}I$ ratios of the iodine carrier are determined to be less than 2×10^{-13}. The analytical precision was less than 5% for all the samples.

The trapping solution was diluted by a factor of 20-50 with 1% $NH_3\cdot H_2O$, and analysed for ^{127}I concentration by ICP-MS (Agilent 8800, USA) using the mode of single quadrupole and no dynamic collision-reaction gas. Cs^+ (CsCl) was used as an internal standard in the ICP-MS measurement of iodine. The sensitivity of ^{127}I is 250 Mcps per 1 mg L^{-1} of iodine, and the instrumental detection limit is 0.002 μg L^{-1} for ^{127}I.

S1.4 Calculation of z-score of ^{129}I concentrations and $^{129}I/^{127}I$ ratios

Z-scores of ^{129}I concentrations and $^{129}I/^{127}I$ ratios are calculated by subtracting the sample mean from an individual raw score and then dividing the difference by the sample standard deviation (Eq.1). The absolute value of z-score represents the distance between the raw ^{129}I concentrations and $^{129}I/^{127}I$ ratios and the sample mean in units of the standard deviation.

$$z = \frac{x-\bar{x}}{s} \quad \text{Eq. (1)}$$

Where, $\bar{x}$ is the mean of the sample; S is the standard deviation of the sample; z is negative when the raw score is below the mean, positive when above.

SI-2 Monthly and seasonal variations

^{127}I and ^{129}I in aerosols are characterized with the apparent monthly and seasonal variations (Fig.S1 and S2). The minimum and maximum of monthly concentrations were observed in August and December for ^{127}I, and July and December for ^{129}I, respectively. ^{127}I concentrations in November, December and January (11.4-12.7 μg m^{-3}) were more than two times higher than those in other months (3.12-6.70 μg m^{-3}). Distinct from ^{127}I, monthly variation of ^{129}I shows the lowest level in June and July ((0.47-0.50) $\times10^5$ atoms m^{-3}), about two to six times lower than other months. The maximum of $^{129}I/^{127}I$ ratio was not observed in winter months but in September.

The mean ^{127}I concentrations were 5.68±2.34 μg m^{-3}, 3.61±1.49 μg m^{-3}, 6.05±4.52 μg m^{-3}, and 10.6±6.0 μg m^{-3} in spring, summer, fall and winter, respectively. The level of ^{127}I in winter was about two times higher than spring and fall, three times higher than summer. ^{129}I were (2.10±1.83) $\times10^5$ atoms m^{-3}, (1.24±1.54) $\times10^5$ atoms m^{-3}, (1.92±1.62) $\times10^5$ atoms m^{-3}, and (4.17±1.37) $\times10^5$ atoms m^{-3} in spring, summer, fall and winter, respectively. The level of ^{129}I in winter was about two times higher than spring and fall, and 3.3 times higher than summer. Seasonal variation of $^{129}I/^{127}I$ ratios was not such obvious as the concentrations of iodine isotopes. The mean $^{129}I/^{127}I$ ratios were (119±185) $\times10^{-10}$ in fall and (124±112) $\times10^{-10}$, slightly higher than those of (87.7±76.5) $\times10^{-10}$ in spring and (75.1±85.1) $\times10^{-10}$ in summer. Whereas, the ratios in all four seasons fell in the similar range as that of the whole year.

SI-3. Influence of precipitation and win speed

Precipitation. Wet and dry deposition are vital pathways of iodine removal from the atmosphere. The effect of rainfall on iodine concentrations in aerosols is not clear. Xi'an is a warm temperate semihumid continental monsoon climate, with annual precipitation of 522.4-719.5 mm. The annual precipitation was 649.0 mm in 2017, and precipitations in September and October were the most months of 98.6 mm and140 mm, respectively, accounting for 37% of the annual precipitation (Fig.2e) (Xi'an Bureau of Statistics, 2018). Taking the two months for exampling, sixteen aerosols were analysed with eight in rainy days and eight in non-rainy days. ^{127}I and ^{129}I concentrations fell in the ranges of 1.88-4.93 ng m^{-3} and (1.88-4.93) $\times 10^5$ atoms m^{-3} in rainy days, respectively, were comparable to 1.67-8.22 ng m^{-3} and (0.44-7.25) $\times 10^5$ atoms m^{-3} in non-rainy days. Although the concentration range was narrower in rainy days than non-rainy days, the data in same range suggest that precipitation does not significantly affect the variation of both iodine isotopes in aerosols. Furthermore, this conclusion is also supported by the fact that the frequent rainfall in October did not change iodine concentrations.

Wind speed. Wind speed affect not only the sources of iodine, but also the dispersion rate and retention in local atmospheric system. Controlled by topography, the annually prevailing wind direction is northeasterly wind in Xi'an and daily average wind speed was 1.0-4.1 m s^{-1} during the studied periods. ^{127}I and ^{129}I varied irregularly with changes of wind speed throughout the year (Fig.2f). These data indicated that small-scale atmospheric circulation limited within a local area unlikely had regular influence on variations of iodine isotopes, which is identical to the observation in Risø, Denmark (Zhang et al., 2016). Large-scale atmospheric circulation, however, might be profound, which will be discussed in the following section.

SI-4. Quantitative characterization of the influence of EAM on variation of ^{129}I

To quantitatively characterize the influence of EAM on variation of ^{129}I, z-normalized ^{129}I concentrations and $^{129}I/^{127}I$ ratios were used to build a quantitative model during winter monsoon and different stages of the summer monsoon including onset, active, break, revival and retreat (Fig.S8S). Z(^{129}I) varies from -1.11 to 3.38 with a median value of -0.29, and z($^{129}I/^{127}I$ ratio) from -0.66 to 5.26 with a median value of -0.34. Based on the observation during 2017/2018 in the Guanzhong Basin, when z(^{129}I) is less than -0.5 and z($^{129}I/^{127}I$ ratio) is smaller than 0, this period is in good agreement with the onset, active and revival stages of the EASM. During the stable active-stage, z-scores for ^{129}I and $^{129}I/^{127}I$ were minimal, which was followed by the second lowest value during the revival stage. The onset and break stage showed much larger fluctuation with z-scores changing from -0.8 to -0.3. The break stage of East Asia summer monsoon is an exception, which exists alternative influence from both factors in our studied region. The z(^{129}I) from 1.57 to 1.96 of the break stages were even much higher than the period controlled by East Asia winter monsoon with z(^{129}I) from -0.5 to 1.53.

Reference

Hou, X., Zhou, W., Chen, N., Zhang, L., Liu, Q., Luo, M., Fan, Y., Liang, W. and Fu, Y.: Determination of ultralow level $^{129}I/^{127}I$ in natural samples by separation of microgram carrier free iodine and accelerator mass spectrometry detection, Anal. Chem., 82(18), doi:10.1021/ac101558k, 2010.

Xi'an Bureau of Statistics: Xi'an Statistics Yearbook. [online] Available from: http://tjj.xa.gov.cn/ptl/def/def/2017/zk/indexch.htm, 2018.

Zhang, L., Hou, X. and Xu, S.: Speciation of ^{127}I and ^{129}I in atmospheric aerosols at Risø, Denmark: Insight into sources of iodine isotopes and their species transformations, Atmos. Chem. Phys., 16, 1971–1985, 2016.

Zhang, L., Hou, X., Fu, Y., Fang, M. and Chen, N.: Determination of ^{129}I in aerosols using pyrolysis and AgI–AgCl coprecipitation separation and accelerator mass spectrometry measurements, J. Anal. At. Spectrom., 33, 1729–1736, doi:10.1039/C8JA00248G, 2018b.

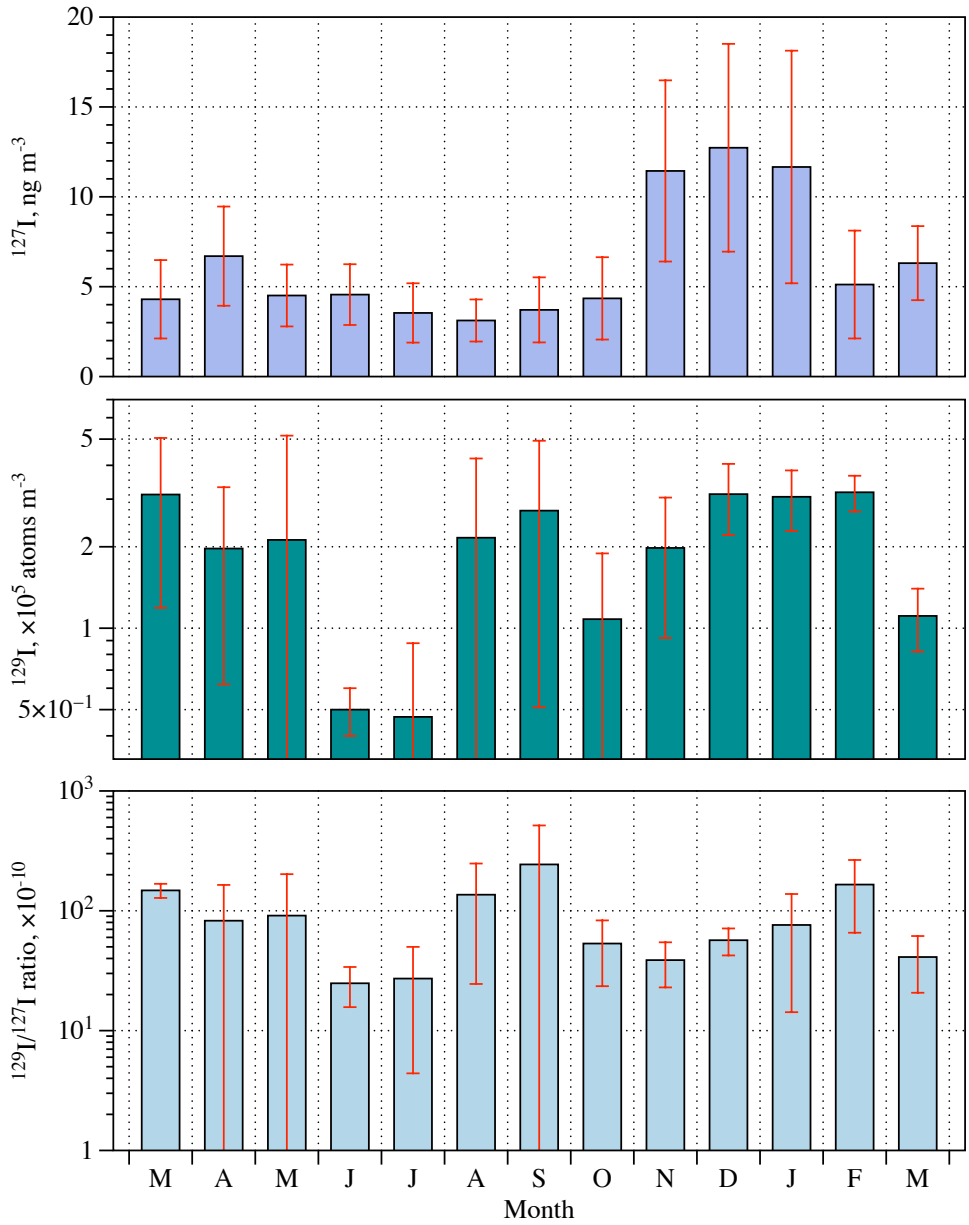

Fig. S1 Monthly variation of ^{127}I (a), ^{129}I concentrations (b) and ^{129}I/^{127}I ratios (c) in aerosols from March 2017 to March 2018.

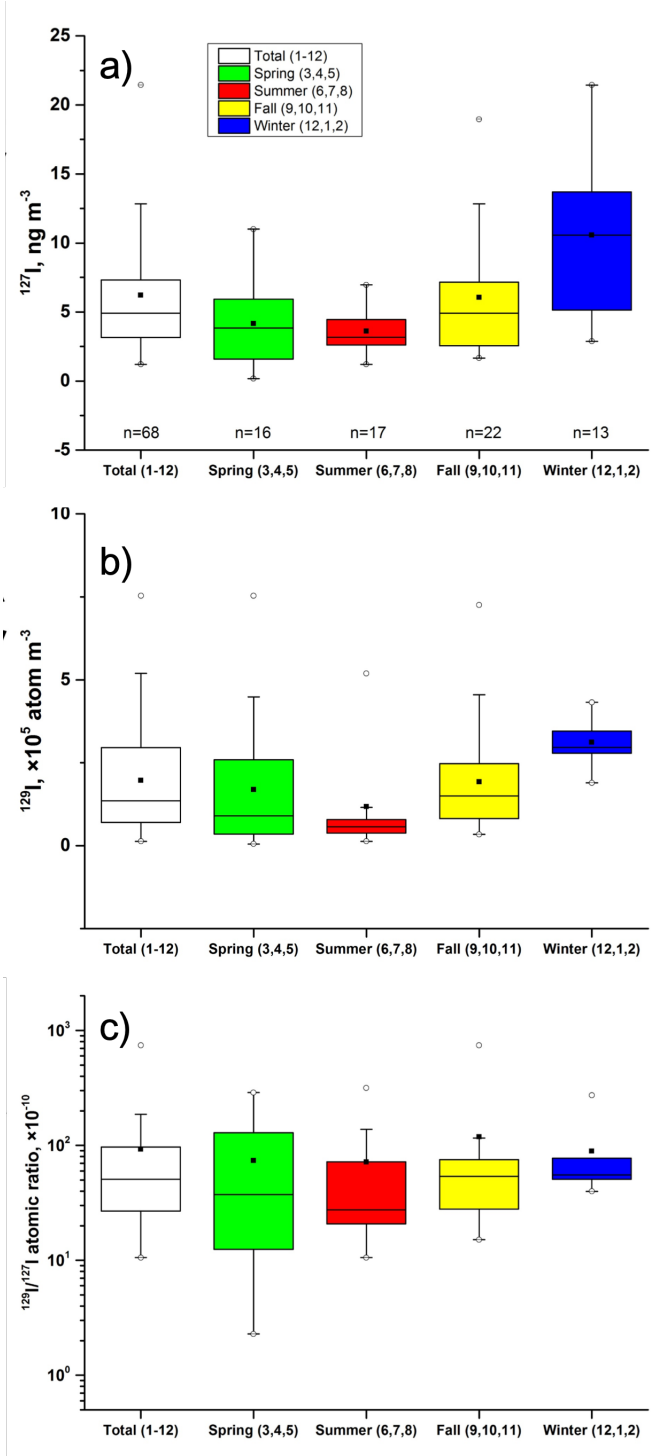

Fig. S2 Seasonal variation of ^{127}I (a), ^{129}I (b) and ^{129}I/^{127}I atomic ratios (c) in aerosols collected in Xi'an, China from March 2017 to March 2018. The boxes show the range from 25% to 75%. Mean and median values are indicated with black solid squares and horizontal bars, respectively. The whisker indicates the upper and lower limits excluding outliers shown by dots. The outliers are defined as those 1.5 times greater than the interquartile range.

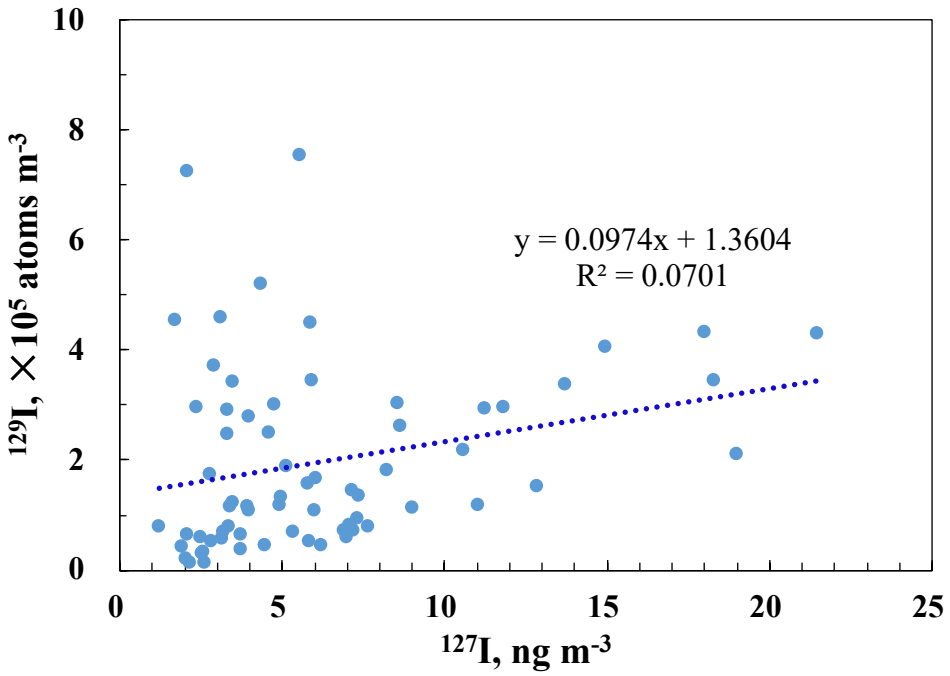

Fig. S3 Relationship between ^{127}I and ^{129}I, showing no significant correlation (R=0.265) between the two iodine isotopes. This indicates the two iodine isotopes have different sources and their temporal variation patterns were affected by different factors.

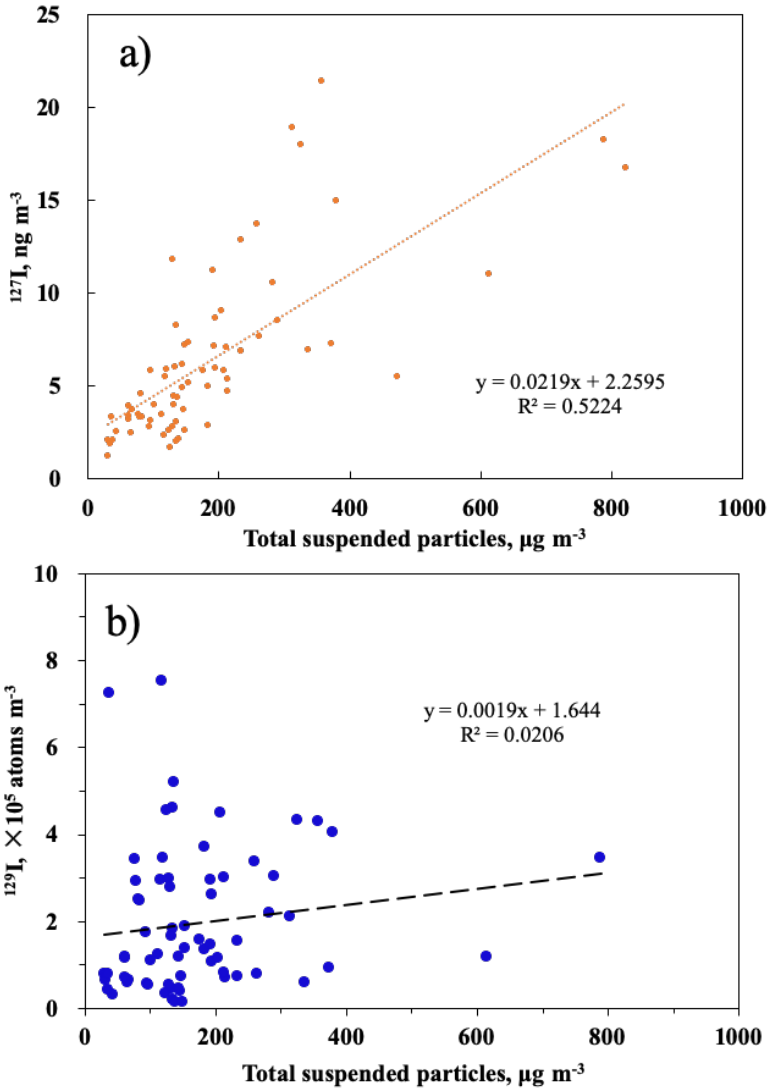

Fig. S4 Relationship between iodine isotopes and total suspended particles (TSP) in Xi'an, China (n=68), suggesting significant correlation between ^{127}I and TSP, and no correlation between ^{129}I and TSP. The results indicate ^{127}I was sourced from local input and ^{129}I was transported to the studied site externally.

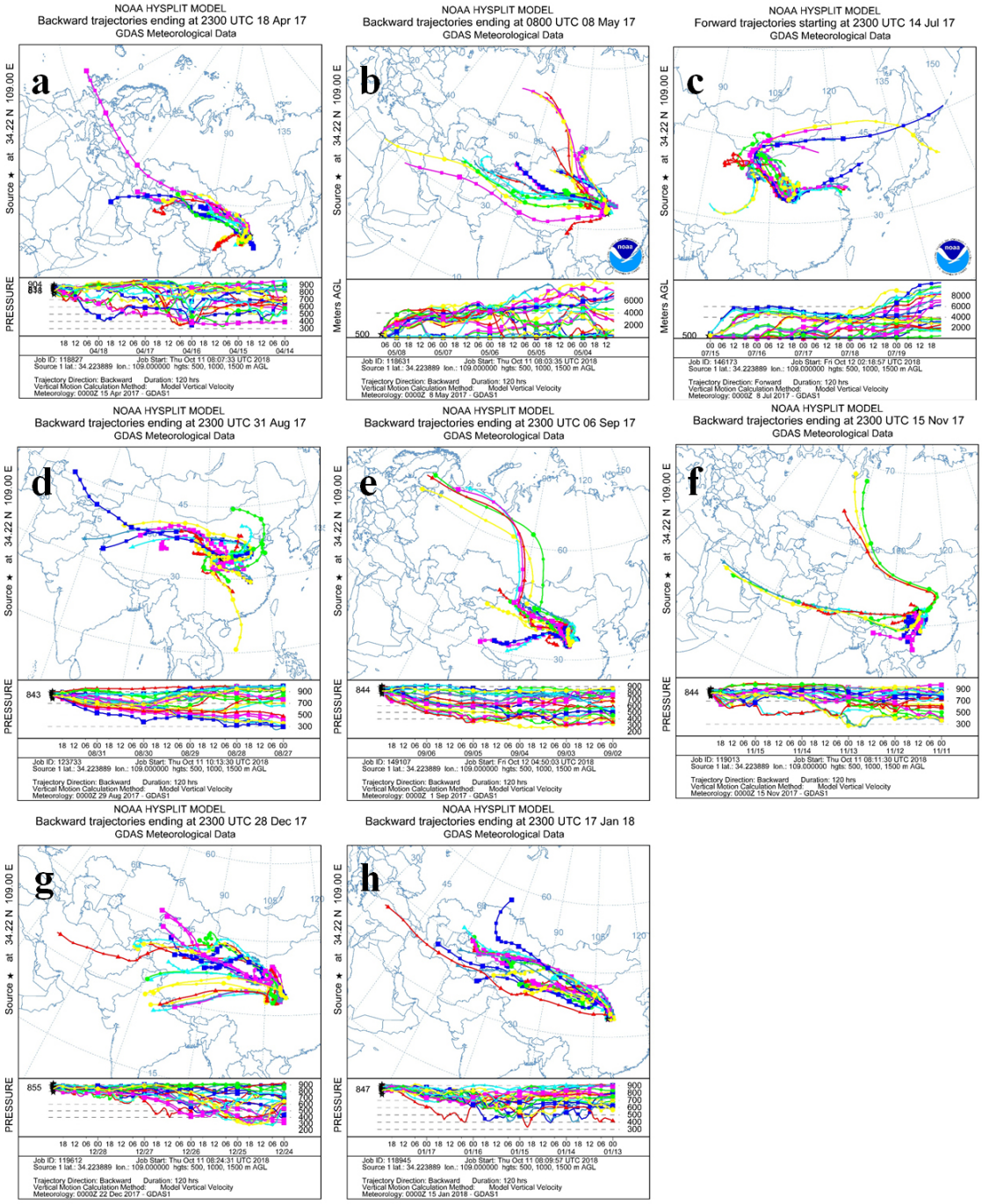

Fig. S5 Back trajectories analyisis on date of a) 18th April, 2017; b) 18th May, 2017; c) 14th July, 2017; d) 31st August, 2017; e) 6th September, 2017; f) 15th November, 2017; g) 28th December, 2017; h) 17th January, 2018.

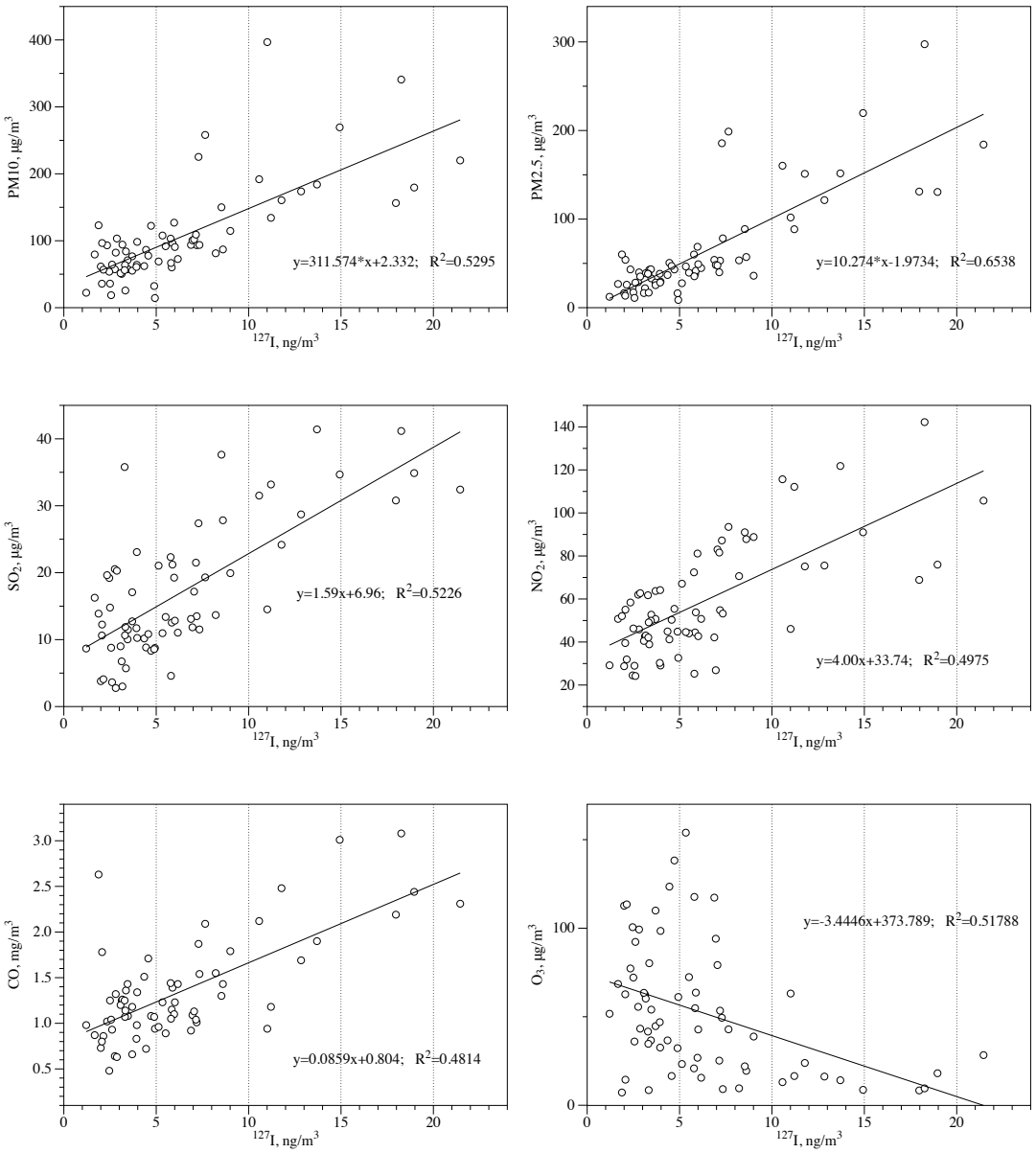

130

Fig. S6 Relations between ^{127}I and air pollutants including PM10, PM2.5, SO_2, NO_2, CO and O_3, showing significant correlation.

135

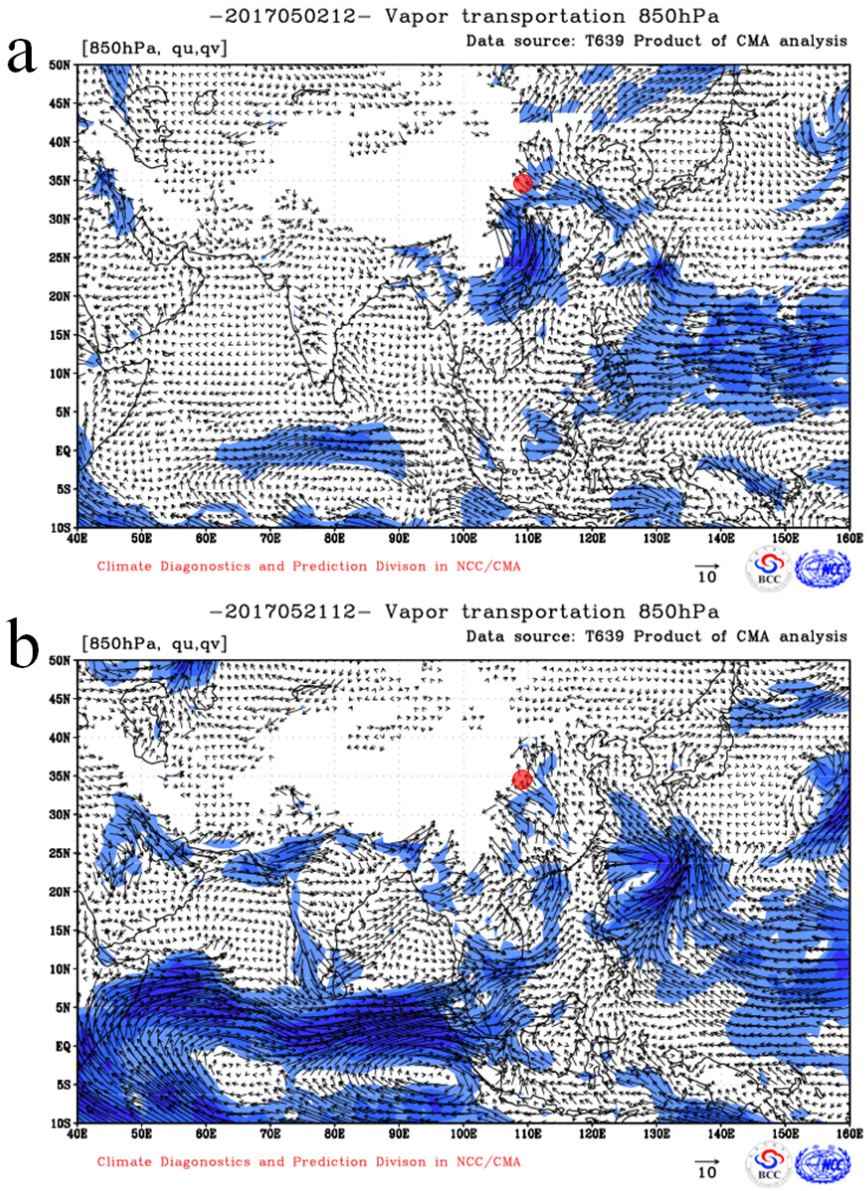

Fig. S7 850 hPa water vapor transmission flow field on 2 May, 2017 (a), and 21 May, 2017 (b). Data from: https://cmdp.ncc-cma.net/Monitoring/monsoon.php?ListElem=vt85. The red dot in the figures is the sampling location, Xi'an, China.

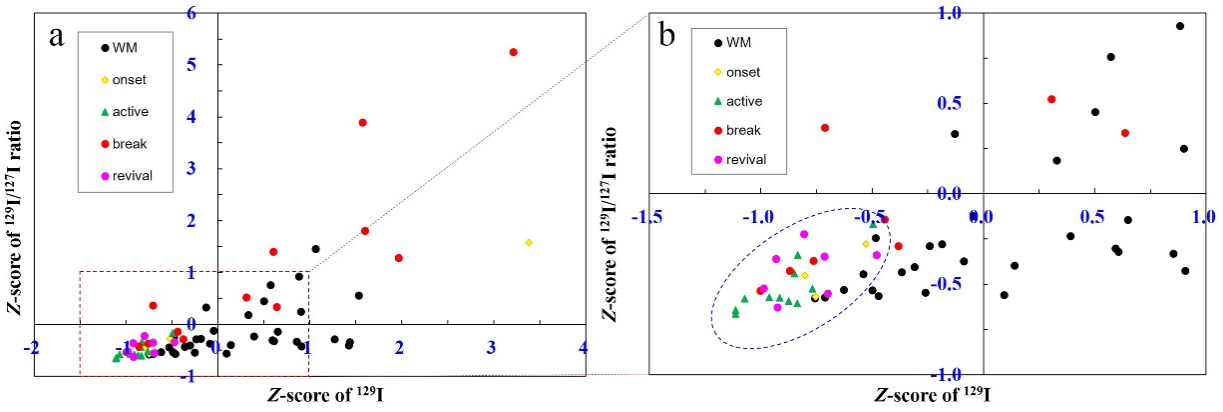

140

Fig. S8 Two-dimension graph of z-score normalized ^{129}I concentrations and $^{129}I/^{127}I$ ratios, suggesting the refined features of East Asia summer (onset, active, break and revival in yellow diamond, green triangle, red circle and pink circle, respectively) and winter monsoons (WM, black dot) (a). The colored symbols clearly demonstrate a detailed cycle of onset-active-break-revival for the summer monsoon with $Z_{129I} \leq -0.5$ and $Z_{Ratio} \leq 0$, as illustrated in the blue oval area (b).

145

Table S1 Iodine isotopes in aerosols from Xi'an, China from March 2017 to March 2018

No	Date	^{127}I, ng/m^3	^{129}I, × 10^5 atom/m^3	$^{129}I/^{127}I$ atomic ratio, ×10^{-10}
1	2017-3-30	2.76 ± 0.15	4.49 ± 0.15	162 ± 7
2	2017-4-1	5.97 ± 0.06	1.75 ± 0.05	134 ± 4
3	2017-4-3	7.19 ± 0.47	1.07 ± 0.09	38.0 ± 3.3
4	2017-4-4	3.47 ± 0.06	0.72 ± 0.10	21.1 ± 3.0
5	2017-4-11	11.01 ± 0.06	3.42 ± 0.10	208 ± 7
6	2017-4-18	5.88 ± 0.07	1.19 ± 0.08	22.8 ± 1.7
7	2017-4-27	3.97 ± 0.13	3.45 ± 0.12	124 ± 4
8	2017-5-2	5.51 ± 0.05	1.10 ± 0.04	58.2 ± 2.3
9	2017-5-8	3.70 ± 0.06	7.53 ± 0.17	288 ± 7
10	2017-5-15	6.88 ± 0.07	0.64 ± 0.03	36.7 ± 1.9
11	2017.5.21-22	2.46 ± 0.03	1.13 ± 0.13	34.5 ± 5.8
12	2017-5-23	6.96 ± 0.06	0.59 ± 0.02	50.7 ± 2.0
13	2017-6-3	3.13 ± 0.08	0.59 ± 0.10	17.8 ± 3.2
14	2017-6-11	4.45 ± 0.06	0.57 ± 0.03	38.3 ± 2.0
15	2017-6-17	3.70 ± 0.07	0.46 ± 0.04	21.6 ± 1.7
16	2017-6-25	5.34 ± 0.13	0.38 ± 0.02	21.7 ± 1.1
17	2017-7-3	3.36 ± 0.05	0.70 ± 0.04	27.6 ± 1.8
18	2017.7.5-6	2.00 ± 0.05	1.67 ± 0.07	104 ± 6
19	2017-7-14	5.80 ± 0.16	0.20 ± 0.02	20.8 ± 1.7
20	2017.7.16-17	2.14 ± 0.05	0.75 ± 0.06	27.4 ± 3.1
21	2017-7-20	2.61 ± 0.05	0.13 ± 0.02	13.0 ± 2.1
22	2017-7-25	4.72 ± 0.05	0.13 ± 0.02	10.6 ± 1.6
23	2017-8-4	3.17 ± 0.06	3.01 ± 0.07	134 ± 4
24	2017.8.6-7	3.07 ± 0.05	1.01 ± 0.04	67.3 ± 3.9
25	2017-8-11	2.81 ± 0.05	4.60 ± 0.12	316 ± 10
26	2017-8-16	4.35 ± 0.22	0.53 ± 0.04	39.9 ± 2.9
27	2017-8-26	1.21 ± 0.05	5.19 ± 0.56	252 ± 27
28	2017-8-29	2.50 ± 0.13	0.79 ± 0.03	138 ± 6
29	2017-8-31	3.45 ± 0.10	0.31 ± 0.01	26.5 ± 1.4
30	2017-9-2	3.31 ± 0.05	1.23 ± 0.07	75.4 ± 4.6
31	2017-9-4	2.06 ± 0.30	2.47 ± 0.07	157 ± 5
32	2017-9-6	4.93 ± 0.30	7.25 ± 0.28	743 ± 39
33	2017-9-9	1.67 ± 0.11	1.33 ± 0.05	57.0 ± 2.6
34	2017-9-11	2.34 ± 0.1	4.55 ± 0.14	575 ± 24
35	2017-9-12	7.05 ± 0.05	2.96 ± 0.06	266 ± 8
36	2017-9-21	4.89 ± 0.4	0.81 ± 0.05	24.3 ± 1.6
37	2017-9-27	2.07 ± 0.07	1.17 ± 0.21	50.6 ± 9.0
38	2017-10-2	2.56 ± 0.2	0.64 ± 0.03	65.0 ± 3.6
39	2017-10-4	6.17 ± 1.0	0.34 ± 0.02	27.9 ± 1.8
40	2017-10-6	1.88 ± 0.6	0.44 ± 0.03	15.1 ± 1.1
41	2017-10-8	3.33 ± 1.0	0.43 ± 0.02	48.1 ± 2.9
42	2017-10-11	8.22 ± 2.1	0.79 ± 0.06	49.9 ± 4.0

43	2017-10-13	4.57	±	0.8	1.82	±	0.04	46.6	±	1.7
44	2017-10-16	6.01	±	0.29	2.51	±	0.13	116	±	6
45	2017-10-24	7.15	±	0.33	1.66	±	0.19	58.1	±	6.7
46	2017-11-3	9.01	±	0.64	1.45	±	0.11	42.8	±	3.4
47	2017-11-7	19.0	±	0.12	1.14	±	0.07	26.7	±	1.7
48	2017-11-15	14.9	±	0.39	2.12	±	0.30	23.5	±	3.3
49	2017-11-17	5.78	±	0.17	4.05	±	0.59	57.2	±	8.5
50	2017-11-21	12.8	±	0.73	1.57	±	0.06	57.1	±	2.5
51	2017-11-29	5.13	±	0.42	1.54	±	0.16	25.2	±	2.6
52	2017-12-8	18.0	±	0.15	1.89	±	0.07	77.6	±	2.9
53	2017-12-14	8.61	±	0.06	4.32	±	0.74	50.7	±	8.7
54	2017-12-20	13.7	±	0.47	2.61	±	0.11	63.9	±	2.8
55	2017-12-22	18.3	±	0.06	3.37	±	0.31	51.9	±	4.8
56	2017-12-28	11.8	±	0.06	3.46	±	0.32	39.9	±	4.2
57	2018.1.6-7	11.2	±	0.07	4.28	±	0.19	76.6	±	5.0
58	2018.1.11-12	21.4	±	0.13	4.58	±	0.39	86.1	±	10.4
59	2018.1.16-17	10.6	±	0.05	7.33	±	0.36	72.1	±	8.0
60	2018.1.22-23	3.29	±	0.06	3.54	±	0.28	70.6	±	7.9
61	2018.1.29-30	3.95	±	0.07	4.09	±	0.32	262	±	31
62	2018.2.3-4	8.53	±	0.03	4.05	±	0.32	216	±	25
63	2018.2.8-9	2.87	±	0.06	4.96	±	0.38	123	±	13
64	2018.2.11-12	7.29	±	0.08	5.78	±	0.21	424	±	24
65	2018.3.3-4	3.93	±	0.06	1.60	±	0.11	46.3	±	3.9
66	2018.3.6-7	7.65	±	0.07	1.63	±	0.07	87.6	±	5.3
67	2018.3.12-13	7.34	±	0.13	1.26	±	0.16	34.8	±	5.6
68	2018.3.19-20	2.76	±	0.05	2.01	±	0.15	57.7	±	5.3

Table S2 Mean ^{129}I concentrations and $^{129}I/^{127}I$ ratios in three high-level periods (HLP) and two low-level periods (LLP)

No	Type	Start date	Stop date	^{129}I, $\times 10^5$ atoms/m^3		$^{129}I/^{127}I$ atomic ratio, $\times 10^{-10}$		Monsoon stage
				Average	RSD	Average	RSD	
1	HLP 1	28 Mar, 2017	22 May, 2017	2.37	91%	101.30	89%	WM and onset of SM
2	LLP 1	23 May, 2017	25 Jul, 2017	0.49	60%	28.47	65%	Active of SM
3	HLP 2	4 Aug, 2017	12 Sep, 2017	1.98	109%	155.45	141%	Break of SM
4	LLP 2	21 Sep, 2017	11 Oct, 2017	0.66	44%	40.15	44%	Revival of SM
5	HLP 3	13 Oct, 2017	20 Mar, 2018	2.41	44%	67.87	83%	SM retreat and WM advance then active